Correlation between Modulus Relaxation and Excess Entropy in Pd-Based Metallic Glasses

Jing-Bo Cui(崔静波)[1], Guang-Hui Xing (邢光辉)[1], Guo-Jian Lyu (吕国建)[1,2*],Yun-Jiang Wang (王云江) [3,4] , Takeshi Wada[5], Hidemi Kato[5], Vitaly A. Khonik[6], Yong-Yang (杨勇) [7,8], and Ji-Chao Qiao (乔吉超) [1,9*]

[1]School of Mechanics and Transportation Engineering, Northwestern Polytechnical University, Xi'an 710072, China

[2]Chongqing Innovation Center, Northwestern Polytechnical University, Chongqing, 401135, China

[3]State Key Laboratory of Nonlinear Mechanics, Institute of Mechanics, Chinese Academy of Sciences, Beijing 100190, China

[4]School of Engineering Science, University of Chinese Academy of Sciences, Beijing 100049, China

[5]Institute for Materials Research, Tohoku University, Sendai, 980-8577, Japan

[6]Department of General Physics, Voronezh State Pedagogical University, Lenin Street 86, Voronezh 394043, Russia

[7]Department of Mechanical Engineering, College of Engineering, City University of Hong Kong, Tat Chee Avenue, Kowloon Tong, Kowloon, Hong Kong SAR, China

[8]Department of Materials Science and Engineering, College of Engineering, City University of Hong Kong, Tat Chee Avenue, Kowloon Tong, Kowloon, Hong Kong SAR, China

[9]State Key Laboratory of Clean and Efficient Turbomachinery Power Equipment, Northwestern Polytechnical University, Xi'an, 710072, China

* Corresponding authors at: School of Mechanics and Transportation Engineering, Northwestern Polytechnical University, Xi'an 710072, China.

Corresponding author. Email: qjczy@nwpu.edu.cn (J.C. Qiao)

guojian.lyu@nwpu.edu.cn (G.J. Lyu)

Abstract

The correlation between structural disorder and relaxation behavior in metallic glasses (MGs) plays a key role in governing their glass transition and viscoelastic response. In this work, differential scanning calorimetry and dynamic mechanical analysis were employed to systematically investigate the thermodynamic and relaxation behaviors of $Pd_{40}Ni_{40}P_{20}$ and $Pd_{20}Pt_{20}Cu_{20}Ni_{20}P_{20}$ MGs. The temperature dependent evolutions of the excess entropy, complex modulus, and relaxation modulus analyzed over a wide temperature range. A dimensionless disorder parameter ξ was introduced, and its correlation with relaxation kinetics was demonstrated. The results show that, compared with $Pd_{40}Ni_{40}P_{20}$ MG, $Pd_{20}Pt_{20}Cu_{20}Ni_{20}P_{20}$ MG exhibits higher structural disorder and more active relaxation kinetics. This study contributes to understanding the relationship between structural disorder and relaxation behavior in MGs and their connection to compositional design.

Keywords: metallic glass, relaxation, modulus, excess entropy, disorder

PACS: 64.70.Pe, 62.40.+i, 62.20.-x.

1. Introduction

Amorphous materials, due to their intrinsic structural disorder, exhibit complex relaxation behavior. [1–3] However, this inherent disorder hinders the establishment of universal thermodynamic–kinetic correlations, thereby posing a fundamental challenge for understanding and designing amorphous solids. In amorphous systems, continuous structural relaxation toward thermodynamic equilibrium results in pronounced time dependent evolution of physical properties, while the underlying complex dynamics play a critical role in governing their macroscopic responses. [4–6] Metallic glasses (MGs), whose atomic configurations can be approximated as densely packed random hard spheres, are widely regarded as ideal model systems for investigating the relationship between thermodynamics and kinetics in amorphous solids. [7–9]

Among the various physical properties of MGs, the modulus is an important parameter closely associated with glass transition, structural relaxation, and crystallization behaviors. [10,11] Previous studies have shown that both relaxation and crystallization are typically accompanied by pronounced thermal events, together with variations in the modulus. [12,13] Meanwhile, the excess entropy ΔS, defined as the entropy difference between the glassy and crystalline states, serves as a quantitative measure of structural disorder. [14-16] Previous study has shown that ΔS is closely related to dynamic processes in amorphous solids. [17] Establishing a direct relationship between modulus relaxation kinetics and ΔS, which characterizes the configurational state of the system, represents a fundamental scientific challenge. Addressing this issue is crucial for elucidating the evolution of the energy landscape and the kinetic stability of amorphous systems.

Although relaxation behavior in MGs has been extensively studied, a quantitative correlation between thermodynamic properties and relaxation dynamics remains insufficiently established. [18,19] Moreover, identifying an appropriate thermodynamic parameter to characterize relaxation behavior is still an open question. In this work, $Pd_{40}Ni_{40}P_{20}$ and $Pd_{20}Pt_{20}Cu_{20}Ni_{20}P_{20}$ MGs were selected as model systems due to their excellent thermal stability. The temperature dependent ΔS was determined by differential scanning calorimetry, while modulus relaxation behaviors were systematically characterized using dynamic mechanical analysis. A notable correlation is observed between the change rate of modulus evolution and the variation in ΔS. Based on this relationship, a dimensionless parameter ξ derived from ΔS is

introduced [20], providing a metric for the modulus relaxation kinetics. Near the glass transition temperature (T_g), a larger value of ξ corresponds to more pronounced modulus decay and faster relaxation kinetics. These findings contribute to the understanding of the relationship between thermodynamics and kinetics in amorphous solids.

2. Experimental procedure

The $Pd_{40}Ni_{40}P_{20}$ and $Pd_{20}Pt_{20}Cu_{20}Ni_{20}P_{20}$ alloys were prepared via the B_2O_3 fluxing method, followed by melt spinning under an argon atmosphere to produce amorphous ribbons. [21] The thermal properties of the $Pd_{40}Ni_{40}P_{20}$ and $Pd_{20}Pt_{20}Cu_{20}Ni_{20}P_{20}$ MGs were characterized using a differential scanning calorimeter (DSC, Hitachi 7020) under a high-purity nitrogen atmosphere at a heating rate of 5 K/min. The excess entropy ΔS was determined from the DSC thermograms measured at 5 K/min for glassy samples. ΔS was evaluated by integrating the difference in heat flow between the glassy and crystalline states according to the following relation: $\Delta S = \frac{1}{\dot{T}} \int_{T}^{T_{cr}} \frac{\Delta W(T)}{T} dT$, where $\dot{T}$ is the heating rate, T_{cr} is the temperature of the complete crystallization, and $\Delta W = W_{gl} - W_{cr}$ represents the heat flow difference between the glassy state (W_{gl}) and the crystalline state (W_{cr}). [15,22]

Dynamic relaxation measurements of the $Pd_{40}Ni_{40}P_{20}$ and $Pd_{20}Pt_{20}Cu_{20}Ni_{20}P_{20}$ MGs were carried out using a dynamic mechanical analyzer (TA Instruments 850) in tensile film mode. Under a sinusoidal stress $\sigma(t) = \sigma_0 \sin(2\pi ft)$, the corresponding strain response can be written as $\varepsilon(t) = \varepsilon_0 \sin(2\pi ft - \theta)$, where f denotes the frequency and θ represents the phase lag between stress and strain. The complex modulus is expressed as $E^* = \sigma/\varepsilon = E' + iE''$, where E' is the storage modulus, E'' is the loss modulus. The dynamic relaxation tests were conducted at a frequency of 0.3 Hz with a heating rate of 5 K/min. Isothermal stress relaxation tests were carried out at a constant strain of 0.3% for 1800 s. To reduce the effect of thermal expansion associated with conventional non-isothermal measurements, a multi-step stress relaxation protocol was adopted. In this protocol, stress relaxation tests were performed over a temperature range of $0.55T_g$ to $1.03T_g$ with a step size of $0.01T_g$. At each temperature, a constant strain ε_c of 0.3% was applied, and the corresponding modulus response was recorded for 10 s. Therefore, the relaxation modulus G at each temperature is calculated as $G = \sigma(t = 10\ \text{s})/\varepsilon_c$. To facilitate readability, the key

parameters frequently used in this work, along with their descriptions, are summarized in Table 1.

Table 1 Descriptions of the key parameters used in this work.

Parameter	Description
ΔS	Excess entropy
T_g	Glass transition temperature
ΔS_{T_g}	The excess entropy at T_g
$\Delta S_{\max}$	The maximum value of ΔS
ξ	Dimensionless parameter, $\xi = (\Delta S_{\max} - \Delta S_{T_g})/R$
R	Gas constant
E'	Storage modulus
E''	Loss modulus
$E''\max$	The maximum value of E''
E^*	Complex modulus, $E^* = E' + iE''$
E	The magnitude of complex modulus, $E = \lvert E^* \rvert$
E_0	The magnitude of complex modulus at initial temperature
ΔE	Relaxation depth of E, $\Delta E = 1 - E/E_0$ at a certain temperature
ε_c	The constant strain 0.3% set in the stress relaxation (SR) experiment
G	Relaxation modulus, $G = \sigma/\varepsilon_c$. For multi-step SR, $G = \sigma(t = 10\ \text{s})/\varepsilon_c$ at each temperature; For isothermal 1800 s SR, $G = \sigma/\varepsilon_c$ at each time
G_0	G at initial temperature. $G_0 = \sigma(t = 10\ \text{s})/\varepsilon_c$ at initial temperature
ΔG	Relaxation depth of G. For multi-step SR, $\Delta G = 1 - G/G_0$ at a certain temperature
$G(0)$	For isothermal 1800 s SR, $G(0)$ is the G at initial time
δ	SR strength, for isothermal 1800 s SR, $\delta = 1 - G/G(0)$ at 1800 s
τ_{kww}	Characteristic relaxation time
β_{kww}	Shape parameter

3. Results and discussion

As shown in Fig. 1(a)–(b), the glass transition temperature T_g of $Pd_{40}Ni_{40}P_{20}$ and $Pd_{20}Pt_{20}Cu_{20}Ni_{20}P_{20}$ MGs, measured at a constant heating rate of 5 K/min, are

determined to be 576 K and 570 K, respectively. Fig. 1(c)–(d) present the temperature dependence of ΔS for both MGs, with the room temperature value subtracted to highlight the evolution trend. Taking $Pd_{20}Pt_{20}Cu_{20}Ni_{20}P_{20}$ MG as a representative example, the evolution of ΔS can be divided into three distinct regimes corresponding to different states of the structure. In the low-temperature regime, ΔS remains nearly constant with a slight increase, indicating a frozen glassy state with highly restricted atomic mobility and negligible entropy change. In the intermediate regime below T_g, ΔS increases gradually, reflecting the onset of localized atomic rearrangements associated with β relaxation and short-range structural adjustments involving limited cooperative motion.[23–25] Above T_g, ΔS rises rapidly to a maximum (ΔS_{max}) and then decreases with further heating. This behavior corresponds to α relaxation, where the system enters the supercooled liquid state and long-range cooperative motion markedly enhances structural disorder.[26,27] With continued heating, crystallization occurs, driving the system toward an ordered structure and reducing ΔS.

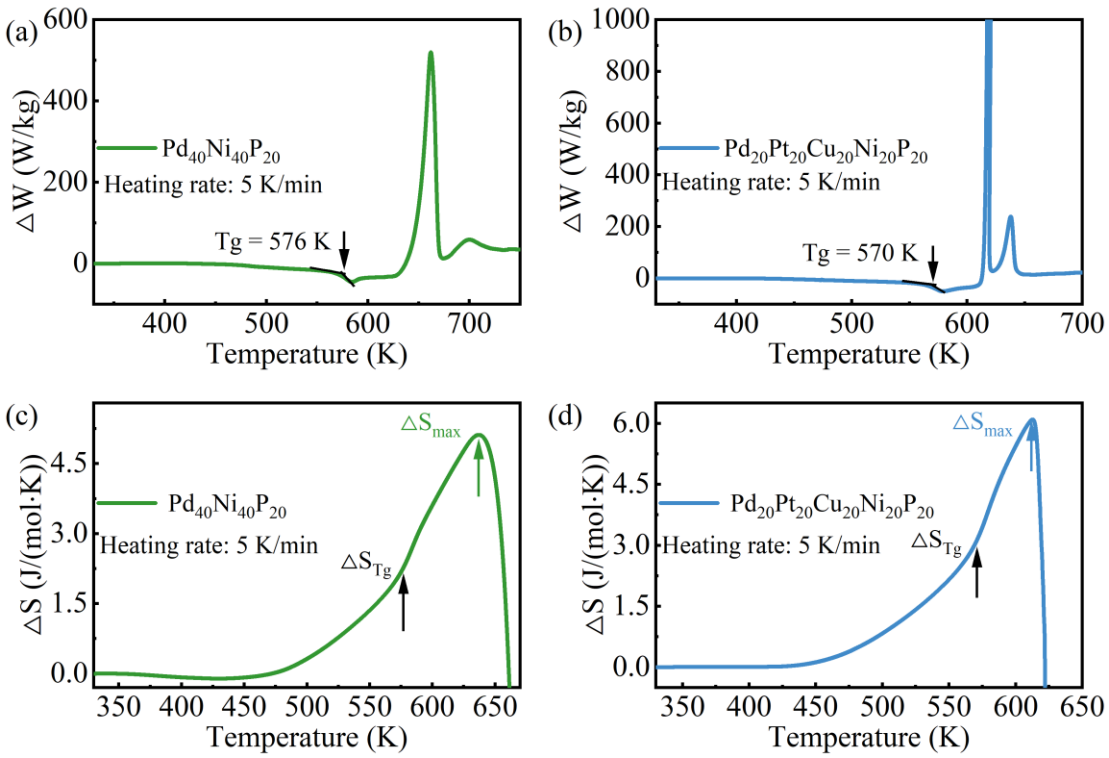


Fig. 1. Heat flow ΔW curves of (a) $Pd_{40}Ni_{40}P_{20}$ and (b) $Pd_{20}Pt_{20}Cu_{20}Ni_{20}P_{20}$ MGs; excess entropy ΔS curves of (c) $Pd_{40}Ni_{40}P_{20}$ and (d) $Pd_{20}Pt_{20}Cu_{20}Ni_{20}P_{20}$ MGs.

Fig. 2 presents the temperature dependent evolution of the normalized complex modulus (E/E_0, where $E = |E^*|$) and normalized relaxation modulus (G/G_0), together with their corresponding rate of change curves, for $Pd_{40}Ni_{40}P_{20}$ and $Pd_{20}Pt_{20}Cu_{20}Ni_{20}P_{20}$

MGs. E_0 and G_0 denote the magnitude of complex modulus and relaxation modulus at the initial temperature, respectively. For $Pd_{20}Pt_{20}Cu_{20}Ni_{20}P_{20}$ MG, E/E_0 remains close to 1 from room temperature to approximately 500 K, indicating a thermally stable glassy state with negligible structural evolution. In the temperature range of 500 K to T_g, E/E_0 decreases progressively, reflecting gradual structural softening. Above T_g, a sharp drop is observed, corresponding to the transition into the supercooled liquid state dominated by long-range cooperative atomic motion. In contrast, G/G_0 exhibits higher sensitivity to temperature, beginning to decrease noticeably at a lower temperature range of 450 - 550 K and decaying rapidly above 550 K. The negative of the derivative of modulus with respect to temperature shows the rate of change of the modulus and can further elucidate the underlying kinetics. These derivatives were calculated directly from the raw experimental data without smoothing. The change rate of complex modulus $-\mathrm{d}(E/E_0)/\mathrm{dT}$ remains near zero below 450 K, then shows a shoulder around 520 K, indicating the activation of β relaxation associated with localized rearrangements and confined cooperative flow units. [28] It reaches a maximum near 594 K, corresponding to α relaxation and macroscopic flow. In comparison, the change rate of relaxation modulus $-\mathrm{d}(G/G_0)/\mathrm{dT}$ exhibits an earlier response, with a shoulder peak signature emerging in the 475 K. Moreover, supplementary normalized loss modulus $E''/E''\mathrm{max}$ curves are presented in Fig. S1. The results show that the shoulder features in $-\mathrm{d}(G/G_0)/\mathrm{dT}$, $-\mathrm{d}(E/E_0)/\mathrm{dT}$, and the $E''/E''\mathrm{max}$ appear within the same temperature range, further validating that the shoulder-shaped peaks in $-\mathrm{d}(G/G_0)/\mathrm{dT}$ and $-\mathrm{d}(E/E_0)/\mathrm{dT}$ correspond to β relaxation. Compared with $Pd_{20}Pt_{20}Cu_{20}Ni_{20}P_{20}$ MG, $Pd_{40}Ni_{40}P_{20}$ MG exhibits a weaker and higher temperature shifted β relaxation feature, which can be attributed to its more positive chemical affinity and consequently weaker atomic interactions, leading to higher energy barriers for local rearrangements and slower relaxation dynamics, consistent with trends observed in loss modulus behavior. [29]

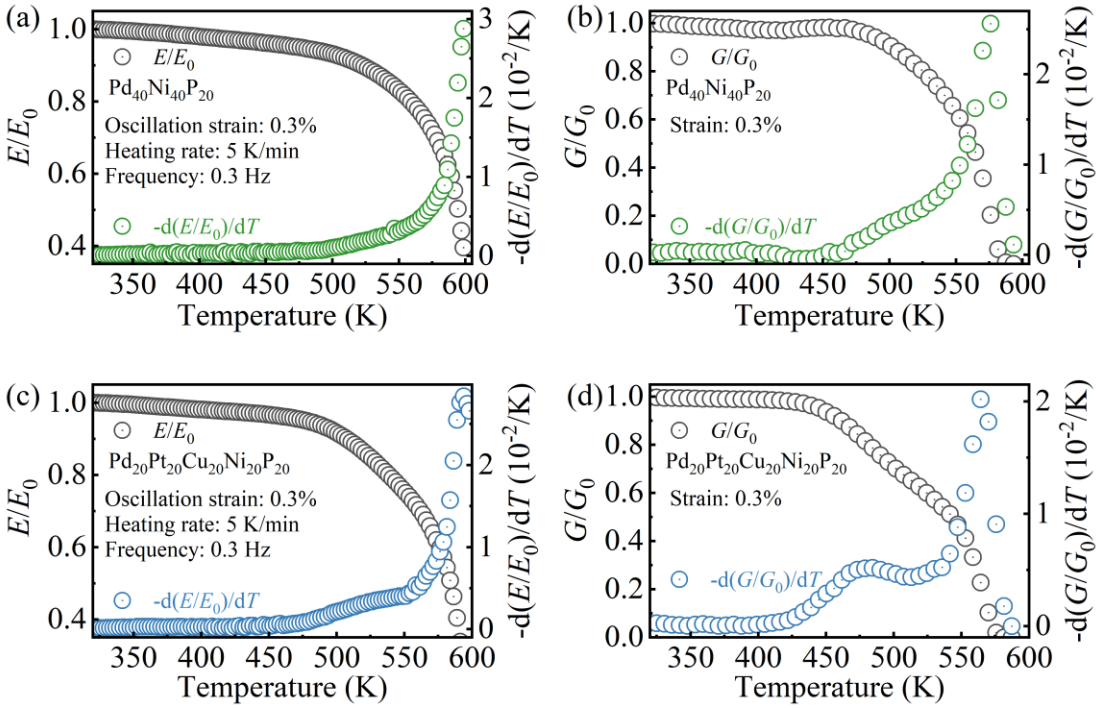


Fig. 2. Temperature dependence of the quantities E/E_0, G/G_0, $-\mathrm{d}(G/G_0)/\mathrm{dT}$, and $-\mathrm{d}(E/E_0)/\mathrm{dT}$ for (a, b) $Pd_{40}Ni_{40}P_{20}$ and (c, d) $Pd_{20}Pt_{20}Cu_{20}Ni_{20}P_{20}$ MGs.

To clarify the correlation between kinetic relaxation and thermodynamic evolution, Fig. 3 presents a comparative analysis of the temperature dependent variations in $-\mathrm{d}(E/E_0)/\mathrm{d}T$, $-\mathrm{d}(G/G_0)/\mathrm{d}T$, and ΔS for $Pd_{40}Ni_{40}P_{20}$ and $Pd_{20}Pt_{20}Cu_{20}Ni_{20}P_{20}$ MGs. Both MGs show a similar evolution across the three quantities, exhibiting a shoulder-shaped feature in the β relaxation regime and a sharp increase above T_g. Clear temperature offsets are also observed among the three responses. Stress relaxation can be regarded as a lower frequency of dynamic mechanical analysis. [30] Consequently, the response of $-\mathrm{d}(G/G_0)/\mathrm{d}T$ appears at the lower temperature, whereas $-\mathrm{d}(E/E_0)/\mathrm{d}T$ evolves at relatively higher temperatures. To further quantify this correlation, the normalized variations of these quantities are presented in Fig. S2. The results indicate a similar temperature evolution for the three quantities. The correlation among these quantities suggests a possible common physical origin governed by the transition from localized rearrangements to long-range cooperative motion. This suggests a coupling between thermodynamic state variables and relaxation kinetics in MGs.

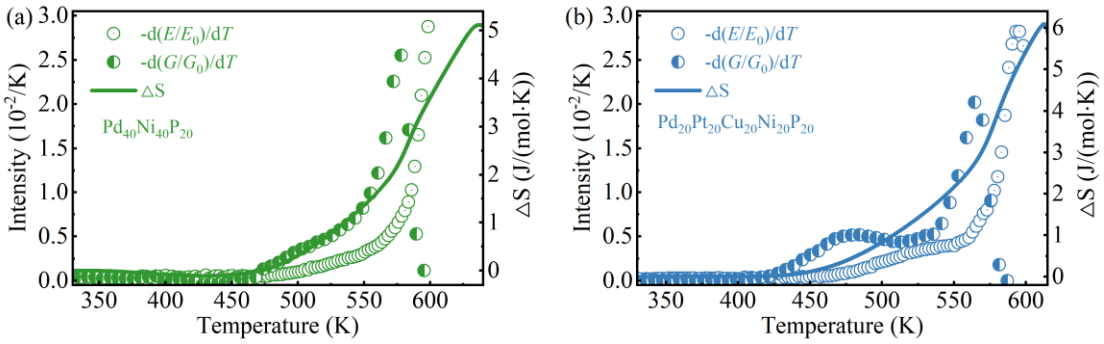
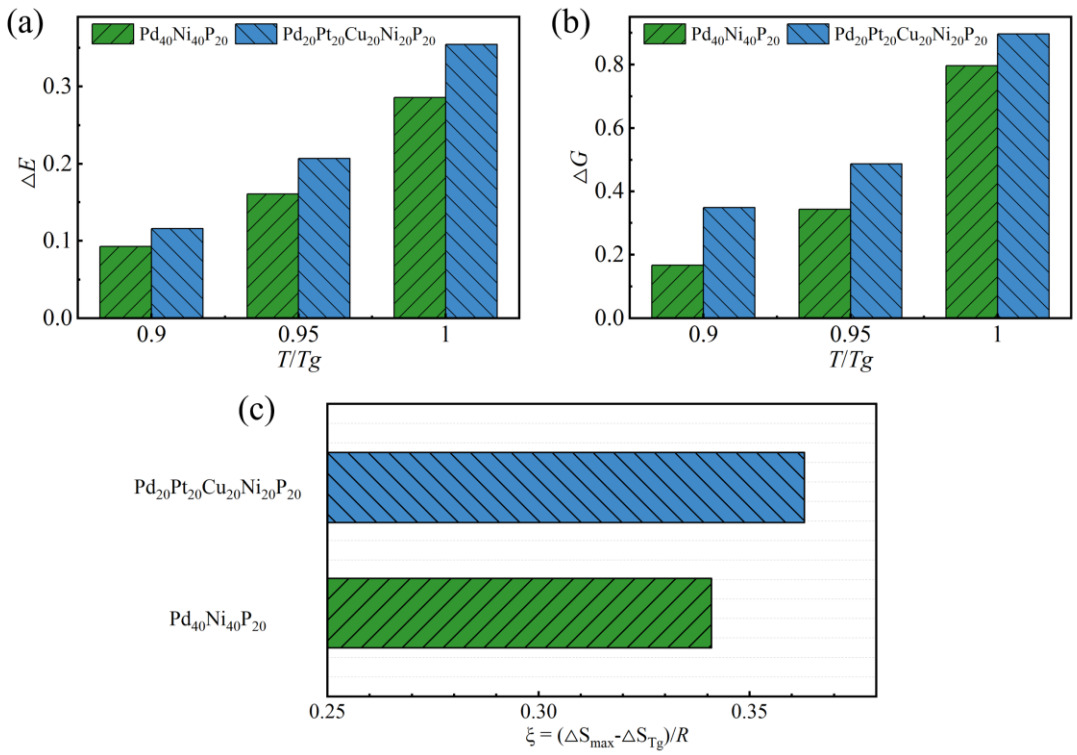


Fig. 3. Temperature dependence of the quantities $-\mathrm{d}(E/E_0)/\mathrm{d}T$, $-\mathrm{d}(G/G_0)/\mathrm{d}T$, and ΔS for (a) $Pd_{40}Ni_{40}P_{20}$ and (b) $Pd_{20}Pt_{20}Cu_{20}Ni_{20}P_{20}$ MGs.

The glass transition is a fundamental process in which amorphous materials transform from a metastable solid to a liquid-like state, influencing microstructural evolution, thermal stability, and mechanical behavior. [31,32] To quantify the link between structural disorder and kinetic response, two parameters are introduced, ΔS_{T_g}, the excess entropy at T_g, and $\Delta S_{\max}$, the excess entropy at the end of the supercooled liquid region, representing the maximum structural disorder of the system. A dimensionless disorder parameter is defined as $\xi = (\Delta S_{\max} - \Delta S_{T_g})/R$, where R is the gas constant. [20] Details of the DSC baseline correction and the protocol used to determine ΔS are given in our previous work. [14] In this study, the estimated uncertainties are around 7 % for ΔS_{T_g} and 1 % for $\Delta S_{\max}$; accordingly, the uncertainty in ξ is governed by that of ΔS_{T_g}. For kinetic characterization, the relaxation depths of the complex modulus and relaxation modulus are defined as $\Delta E = 1 - E/E_0$ and $\Delta G = 1 - G/G_0$, evaluated over $0.9T_g$–T_g (Figs. 4(a)–(b)). Both ΔE and ΔG increase monotonically with temperature, indicating enhanced atomic mobility and progressive activation of flow units. Notably, $Pd_{20}Pt_{20}Cu_{20}Ni_{20}P_{20}$ MG exhibits higher ΔE and ΔG than $Pd_{40}Ni_{40}P_{20}$ MG, consistent with its larger ξ value (Fig. 4(c)). This correspondence indicates that a higher degree of structural disorder leads to a stronger kinetic relaxation response.



225

226 **Fig. 4.** Temperature dependence of (a) ΔE and (b) ΔG for $Pd_{40}Ni_{40}P_{20}$ and
227 $Pd_{20}Pt_{20}Cu_{20}Ni_{20}P_{20}$ MGs; (c) the structural disorder parameter ξ for $Pd_{40}Ni_{40}P_{20}$ and
228 $Pd_{20}Pt_{20}Cu_{20}Ni_{20}P_{20}$ MGs.

229 To further support the conclusions, isothermal stress relaxation experiments were
230 conducted at $0.9T_g$ and $0.95T_g$, under a constant strain of 0.3% for 1800 s. As
231 illustrated in Figs. 5(a)–(b), the normalized stress relaxation curves $G/G(0)$ of
232 $Pd_{40}Ni_{40}P_{20}$ and $Pd_{20}Pt_{20}Cu_{20}Ni_{20}P_{20}$ MGs are compared, where $G(0)$ is the initial
233 relaxation modulus. The results demonstrate that the relaxation curves of
234 $Pd_{20}Pt_{20}Cu_{20}Ni_{20}P_{20}$ MG consistently lie below those of the $Pd_{40}Ni_{40}P_{20}$ MG, reflecting
235 a more pronounced modulus decay and faster relaxation process. Stress relaxation
236 strength δ is defined as $1 - G/G(0)$ at 1800 s. The stress relaxation process can be
237 described by the Kohlrausch-Williams-Watts (KWW) equation: $G/G(0) =$
238 $\exp[-(t/\tau_{\mathrm{kww}})^{\beta_{\mathrm{kww}}}]$. [33] Where τ_{kww} represents the characteristic relaxation time
239 and β_{kww} is shape parameter. A larger β_{kww} value corresponds to a narrower
240 relaxation time distribution; When β_{kww} = 1, the relaxation time distribution behaves
241 Debye relaxation. According to Figs. 5(a)-(b), the KWW equation can describe the
242 stress relaxation curve well for both MGs. Notably, compared to $Pd_{40}Ni_{40}P_{20}$ MG,
243 $Pd_{20}Pt_{20}Cu_{20}Ni_{20}P_{20}$ MG exhibits a smaller β_{kww}, suggesting a broader distribution of
244 relaxation times. As shown in Figs. 5(c)–(d), $Pd_{20}Pt_{20}Cu_{20}Ni_{20}P_{20}$ MG exhibits a larger

δ and a smaller τ_{kww} than $Pd_{40}Ni_{40}P_{20}$ MG. These trends are consistent with the structural disorder parameter ξ, indicating its correlation with relaxation behavior.

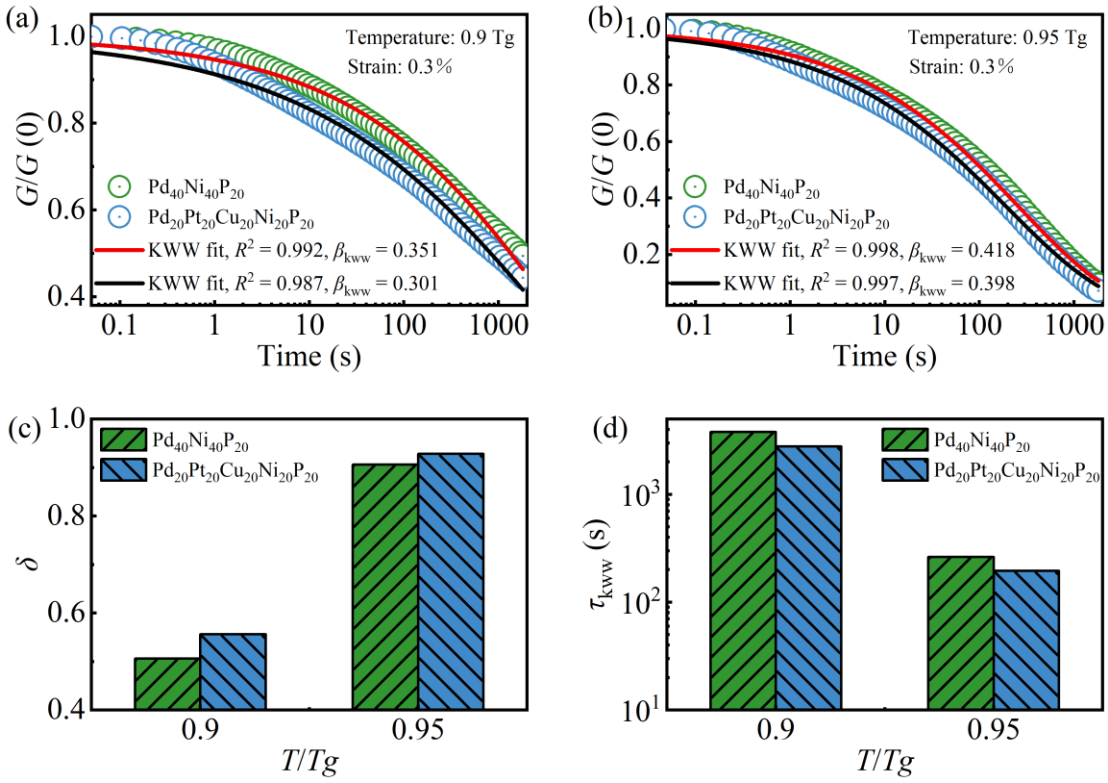


Fig. 5. (a, b) Stress relaxation behavior of $Pd_{40}Ni_{40}P_{20}$ and $Pd_{20}Pt_{20}Cu_{20}Ni_{20}P_{20}$ MGs at $0.9T_g$ and $0.95T_g$, respectively; (c, d) stress relaxation strength δ and characteristic relaxation time τ_{kww} at $0.9T_g$ and $0.95T_g$ for $Pd_{40}Ni_{40}P_{20}$ and $Pd_{20}Pt_{20}Cu_{20}Ni_{20}P_{20}$ MGs.

The correlation between the structural disorder parameter ξ and relaxation kinetics established in this work is closely related to the Adam–Gibbs (AG) theory. The AG theory posits that the structural relaxation time is governed by the configurational entropy, linking the kinetic nature of the glass transition to thermodynamic state variables. [34, 35] In this study, the dimensionless parameter ξ is derived from the excess entropy and quantifies the structural disorder of the system. As shown in Figs. 4 and 5, a larger ξ corresponds to a more pronounced modulus decay and faster relaxation kinetics. This trend is consistent with the thermodynamic description of the AG theory, wherein a higher degree of structural disorder is associated with enhanced atomic mobility, thereby accelerating relaxation. While classical AG analysis primarily focuses on the temperature dependence of viscosity, the parameter ξ introduced here offers a complementary perspective linking excess entropy and modulus relaxation.

The dimensionless parameter ξ employed in this work was originally proposed and validated in our recent study on six MGs, where a correlation with non-isothermal torsional stress relaxation was established. [20] Building on this foundation, the present study further verifies the correlation between ξ and two additional mechanical indicators, specifically the relaxation modulus and the complex modulus. The experimental results confirm that ξ remains closely correlated with both the relaxation modulus and the complex modulus under tensile mode, further verifying the generality of ξ across different testing modes.

4. Conclusion

This study systematically investigates the thermodynamic and kinetic behaviors of $Pd_{40}Ni_{40}P_{20}$ and $Pd_{20}Pt_{20}Cu_{20}Ni_{20}P_{20}$ MGs, revealing the modulus relaxation-excess entropy correlation. The results demonstrate that ΔS, $-\mathrm{d}(E/E_0)/\mathrm{d}T$ and $-\mathrm{d}(G/G_0)/\mathrm{d}T$ exhibit pronounced synergistic evolution. Compared with $Pd_{40}Ni_{40}P_{20}$ MG, $Pd_{20}Pt_{20}Cu_{20}Ni_{20}P_{20}$ MG exhibits higher structural disorder and correspondingly faster relaxation kinetics. These findings contribute to understanding the relationship between structural disorder and relaxation kinetics in MGs. Building on the current study, future work incorporating a broader range of MGs and extensive repeat experiments will be important to further quantify these correlations and explore the underlying mechanisms in greater depth.

Acknowledgements

JCQ is supported by the NSFC (Grant Nos. 52271153 and 12472069) and the Natural Science Foundation of Shaanxi Province (Grant No. 2025GH-YBXM-046). GJL is supported by the NSFC (Grant No. 52301219), the Natural Science Foundation of Chongqing, China (Grant No. CSTB2023NSCQ-MSX0573). YJW acknowledges the financial support by NSFC (Grant No. 12472112). VAK performed the DSC measurements for this study with support from the Russian Science Foundation under the project 23-12-00162. YY is supported by Research Grant Council (RGC), the Hong Kong Government through the General Research Fund (GRF) (Grant Nos. CityU11200719, and CityU11213118).

References

[1] Wang W H 2019 *Prog. Mater. Sci.* **106** 100561

[2] Wang Q, Zhang S T, Yang Y, Dong Y D, Liu C T and Lu J 2015 *Nat. Commun.* **6** 7876
[3] Cui J B, Xing G H, Lyu G J, Wang Y J, Wada T, Kato H, Khonik V A, Yang Y and Qiao J C 2025 *Int. J. Plasticity* **195** 104511
[4] Málek J 2023 *J. Phys. Chem. C* **127** 6080–6087
[5] Shen J, Cornet A, Ronca A, Pineda E, Yang F, Garden J L, Moiroux G, Vaughan G, di Michiel M, Garbarino G, Westermeier F, Goujon C, Legendre M, Liu J, Cangialosi D and Ruta B *Sci. Adv.* **11** eadz7406
[6] Huo J, Li K, Zang B, Gao M, Wang L M, Sun B, Li M, Song L, Wang J Q and Wang W H 2022 *Chinese Phys. Lett.* **39** 046401
[7] Chen Y M, Xiao Y H, Lyu G J, Wang B, Wang Y J, Yang Y, Pineda E, Fusco C, Chazeau L, Qiao J C 2025 *Int. J. Eng. Sci.* **217** 104394
[8] Lu T, Liu S L, Sun Y H, Wang W H and Pan M X 2022 *Chinese Phys. Lett.* **39** 036401
[9] Zhang S, Wang W and Guan P 2021 *Chinese Phys. Lett.* **38** 016802
[10] Wang W H 2012 *Prog. Mater. Sci.* **57** 487–656
[11] Ren N N, Meng T T, Huang H, Ma Q S, Fang J, Li Q and Li W H 2026 *Chinese Phys. B* **35** 016103
[12] Khonik S V, Granato A V, Joncich D M, Pompe A and Khonik V A 2008 *Phys. Rev. Lett.* **100** 065501
[13] Mitrofanov Yu P, Khonik V A, Granato A V, Joncich D M and Khonik S V 2011 *J. Appl. Phys.* **109** 073518
[14] Afonin G V, Qiao J C, Makarov A S, Konchakov R A, Goncharova E V, Kobelev N P and Khonik V A 2024 *Appl. Phys. Lett.* **124** 151905
[15] Makarov A S, Afonin G V, Qiao J C, Glezer A M, Kobelev N P and Khonik V A 2021 *J. Phys-Condens. Mat.* **33** 435701
[16] Smith H L, Li C W, Hoff A, Garrett G R, Kim D S, Yang F C, Lucas M S, Swan-Wood T, Lin J Y Y, Stone M B, Abernathy D L, Demetriou M D and Fultz B 2017 *Nature Phys.* **13** 900–905
[17] Cui J B, Xing G H, Hao Q, Lyu G J, Wang Y J, Wada T, Kato H, Pineda E, Khonik V A and Qiao J C 2026 *Scripta Mater.* **270** 116934
[18] Sun Y T, Zhao R, Ding D W, Liu Y H, Bai H Y, Li M Z and Wang W H 2023 *Nat. Commun.* **14** 540

[19] Sun Y, Peng S X, Yang Q, Zhang F, Yang M H, Wang C Z, Ho K M and Yu H B 2019 *Phys. Rev. Lett.* **123** 105701
[20] Afonin G V, Scherbakov S L, Konchakov R A, Kobelev N P, Cui J B, Qiao J C and Khonik V A 2025 *J. Alloy Compd*. **1048** 185200
[21] Takeuchi A, Chen N, Wada T, Yokoyama Y, Kato H, Inoue A and Yeh J W 2011 *Intermetallics* **19** 1546–1554
[22] Makarov A S, Kretova M A, Afonin G V, Qiao J C, Glezer A M, Kobelev N P and Khonik V A 2022 *JETP Letters* **115** 102–107
[23] Yu H B, Wang W H and Samwer K 2013 *Mater. Today* **16** 183–191
[24] Lu Z, Shang B S, Sun Y T, Zhu Z G, Guan P F, Wang W H and Bai H Y 2016 *J. Chem. Phys*. **144** 144501
[25] Peng S X, Cheng Y, Pries J, Wei S, Yu H B and Wuttig M *Sci. Adv*. **6** eaay6726
[26] Wang Z, Sun B A, Bai H Y and Wang W H 2014 *Nat. Commun*. **5** 5823
[27] Lu Z, Jiao W, Wang W H and Bai H Y 2014 *Phys. Rev. Lett.* **113** 045501
[28] Wang Z and Wang W H 2019 *Natl. Sci. Rev*. **6** 304–323
[29] Yu H B, Samwer K, Wang W H and Bai H Y 2013 *Nat. Commun*. **4** 2204
[30] Xing G, Hao Q, Cui J, Liang S, Wang Y J, Yang Y, Pineda E, Wada T, Kato H and Qiao J 2026 *Newton* 100472
[31] Sun H J, Chang C, Zhou H B, Zhang H P, Jiang M Q and Wang W H 2025 *Phys. Rev. B* **111** 184107
[32] Luan H, Zhang X, Ding H, Zhang F, Luan J H, Jiao Z B, Yang Y C, Bu H, Wang R, Gu J, Shao C, Yu Q, Shao Y, Zeng Q, Chen N, Liu C T and Yao K F 2022 *Nat. Commun*. **13** 2183
[33] Williams G and Watts D C 1970 *Transactions of The Faraday Society* **66** 80-85
[34] Adam G and Gibbs J H 1965 *J. Chem. Phys*. **43** 139-146
[35] Sengupta S, Karmakar S, Dasgupta C, and Sastry S. 2012 Phys. Rev. Lett. **109** 095705